

Fault Injection Attacks on Machine Learning-based Quantum Computer Readout Error Correction

Anthony Etim
Yale University
New Haven, CT, USA
anthony.etim@yale.edu

Jakub Szefer
Northwestern University
Evanston, IL, USA,
jakub.szefer@northwestern.edu

Abstract—Machine-learning (ML) classifiers are increasingly used in quantum computing systems to improve multi-qubit readout discrimination and to mitigate correlated readout errors. These ML classifiers are an integral component of today’s quantum computer’s control and readout stacks. This paper is the first to analyze the susceptibility of such ML classifiers to physical fault-injection which can result in generation of incorrect readout results from quantum computers. The study targets 5-qubit (thus 32-class) readout error-correction model. Using the ChipWhisperer Husky for physical voltage glitching, this work leverages an automated algorithm for scanning the fault injection parameter search space to find various successful faults in all the layers of the target ML model. Across repeated trials, this work finds that fault susceptibility is strongly layer-dependent: early-layers demonstrate higher rates of misprediction when faults are triggered in them, whereas later layers have smaller misprediction rates. This work further characterizes the resulting readout failures at the bitstring level using Hamming-distance and per-bit flip statistics, showing that single-shot glitches can induce structured readout corruption rather than purely random noise. These results motivate treating ML-based quantum computer readout and readout correction as a security-critical component of quantum systems and highlight the need for lightweight, deployment-friendly fault detection and redundancy mechanisms in the quantum computer readout pipelines.

Index Terms—Fault Injection Attacks, Machine Learning, Quantum Computing.

I. INTRODUCTION

Quantum computers rely on measurement of analog signals from qubit readout logic to convert qubit states into classical bitstrings that can be processed by classical computers. While cross-talk errors among qubits and gates have been steadily decreasing due to improvements in quantum computer hardware, the readout errors and noise remain some of the dominant error sources in near-term quantum systems. To mitigate these errors, quantum readout logic increasingly deploys ML-based readout pipelines: from neural discriminators for multiplexed readout to hardware-efficient ML architectures that scale with qubit counts [1], [2]. While these approaches improve fidelity, they also introduce a new security-critical dependency, which is the ML algorithm responsible for performing readout correction operations.

Recent works on the security of the quantum computers highlight that cloud deployment and untrusted classical infrastructure create new threat around the quantum processors [3], [4], [5], [6]. Among existing security analysis of quantum

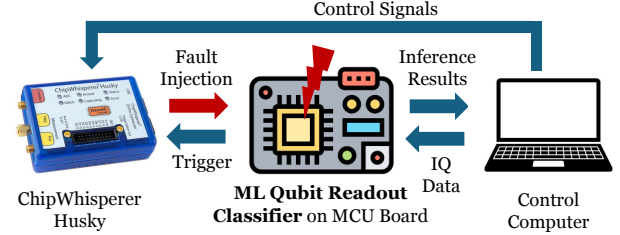


Fig. 1: Overview and setup for evaluation of physical fault injection against ML model that performs quantum computer error correction. The host PC orchestrates inference queries and logging. ChipWhisperer Husky injects a voltage glitches on the target’s supply rail, aligned to a trigger emitted by the target at the start of a chosen neural network layer. Each trial returns a predicted 5-bit class and a status (correct, misprediction, or reset or hang).

computers, readout logic and associated controllers and algorithms are not well understood. To address this research gap, in this paper we focus on one concrete and under-studied area: *physical fault injection* against the ML model that performs quantum computer readout error correction. Overview of the work is given in Figure 1.

Through physical experimentation, in this work we show that a voltage-glitch adversary with physical access to the classical controller can induce mispredictions and create targeted biases in the readout output of a quantum computer. The results are critical as the classical readout is necessary to get the information out of the quantum computer. Results of the quantum computer’s calculations cannot be interpreted if the readout logic causes wrong outputs to be generated. Further, there is a possibility that an attacker can even generate predictable results, thus controlling what output is observed. These physical fault injections can be performed without any modification or changes to the quantum computer as they target the classical quantum computer controllers and ML algorithms embedded in them, and not the qubits that may be hard to access or manipulate, unlike the controller.

A. Introduction to Quantum Measurement and Readout

Quantum computers rely on a classical measurement interface that maps a quantum state to a discrete classical outcomes which are the bits 0 and 1 that can be interpreted by classical logic. In practice, this readout step is noisy due to instrument drift, amplifier noise, crosstalk, and state-preparation-and-measurement (SPAM) effects [7]. Further, readout errors can

be *biased* (e.g., preferentially flipping certain outcomes) and *correlated* across qubits, which is especially consequential for multi-qubit syndrome measurements [8]. As a result, even when gate errors are reduced, measurement error can remain a dominant contributor to logical failure unless explicitly mitigated [9], [10], [6].

B. ML-based Readout Error Correction

Today, ML algorithms are being more frequently leveraged to help with the measurement and readout logic. Deep neural networks can capture non-linear decision boundaries and correlations that arise from multiplexed readout, crosstalk, and non-Gaussian noise, improving discrimination accuracy and calibration robustness [1], [11]. For example, HERQULES emphasizes *hardware-efficient* ML post-processing and scalable deployment, making embedded or near-device execution plausible for low-latency feedback loops [2]. Because such models may sit on the critical path of syndrome extraction and classical control, their integrity is directly tied to the trustworthiness of the overall quantum computation [4], [3].

C. New Fault Injection Attacks on Readout Error Correction

Fault injection in classical systems are known to perturb device operation, e.g., via voltage or clock glitching or electromagnetic pulses, and are able to induce transient computation errors [12], [13], [14]. Further, on ML workloads, faults may corrupt activations, intermediate accumulators, or control flow, potentially causing misclassification, targeted output manipulation, or silent integrity violations [15]. These lessons motivate our evaluation of ML-based readout correction under fault attacks and lead us to *find new fault injection attacks on quantum computer readout and error correction*.

D. Contributions

We present the first hardware fault-injection study of an embedded ML-based quantum readout error-correction model. Our contributions are:

- We formalize a practical physical voltage-glitch adversary against embedded ML-based quantum readout error correction in the quantum–classical control path.
- We implement a repeatable, trigger-synchronized Chip-Whisperer Husky voltage-glitch workflow that localizes injections to specific neural network layers.
- We use Optuna for automated search over glitch parameters to efficiently find high-impact fault settings under constraints.
- We quantify layer-wise susceptibility by reporting best-found configurations and success rates over 96 fault attempts per layer per attack configuration, showing strong layer dependence.
- We characterize integrity degradation showing how specific readout is changed by the faults at each level.

II. THREAT MODEL

A. Victim System and Attack Context

We consider a superconducting quantum computing system in which raw qubit readout generates IQ samples of the

analog signals which are then processed by an ML model to output the correct classical values of the readout. We focus on a superconducting system where the readout logic is shared among qubits. In particular, 5 qubits share one readout line [16]. As the result, the readout logic has to correct for any correlated errors in these bits. This setup is based on existing work which demonstrated a ML algorithm for error correction of the correlated errors [2]. Given there is 5-bit input (from the 5 qubits), there are 32 classes for the ML algorithm to classify the input data into. Our threat model focuses on *the classical controller and embedded processor* that runs this ML inference, and its vulnerability to attacks, consistent with broader concerns that quantum workloads may run atop partially untrusted classical infrastructure [3], [4], [5].

B. Adversary’s Capabilities

We assume an attacker with physical access to the quantum computer controller where the ML algorithm inference is running (e.g., malicious insider, compromised maintenance, or supply-chain attacker with momentary access), enabling transient fault injection through voltage glitching. The attacker can: (i) physically glitch the voltage supply of the controller to induce voltage glitches in the ML algorithm as it executes on the controller, and (ii) synchronize a trigger signal to the execution of the ML inference to cause the short-duration voltage glitches to occur in specific parts of the ML execution.

We assume the attacker has ability to control the glitches parameterized by: `width` or `duration` of the glitch, `intra-cycle offset` of the glitch, `external offset` within the target program (here, the ML algorithm) that determines when the glitch is injected, and `repeat` number of glitches that should be applied. These options are common in platforms such as ChipWhisperer devices [17]. The attacks do not require persistent modification of firmware or stored weights of the ML models. Further, there is no modification to the quantum computing dilution refrigerator or any hardware running at cryogenic temperatures. All attacks are done at the controller, outside of the dilution refrigerator making them much easier than any attacks on components inside the dilution refrigerator.

C. Adversary’s Goals

The attacker’s primary objective is *integrity violation* of corrected readout outputs. We consider two goals:

- **Untargeted Degradation:** reduce the accuracy and increase the Hamming distance between predicted and true 5-bit strings, maximally causing the output to change, leading to incorrect interpretation of the quantum computation’s results.
- **Targeted Steering:** bias corrected outputs toward attacker-chosen bitstrings (specific 5-bit classes), enabling adversarial manipulation of the results of the computation that are received by the users.

D. Assumptions and Out-of-Scope Scenarios

We treat denial-of-service (reset or hang of the controller board) as a secondary outcome (measured but not the only

Algorithm 1 HERQULES neural network forward pass with per-layer cycle windows (MCU cycles). Cycle counts correspond to our C implementation of the algorithm running on ChipWhisperer Husky.

Require: Input vector x

Require: Parameters $\{(W_1, b_1), (W_2, b_2), (W_o, b_o)\}$

Ensure: Output probabilities \hat{y}

```

1:   ▷ Layer 1: Dense 1 executes in cycles [687, 140047]
2:  $z_1 \leftarrow W_1x + b_1$ 
3:   ▷ Layer 2: ReLU 1 executes in cycles [14048, 15602]
4:  $a_1 \leftarrow \max(0, z_1)$ 
5:   ▷ Layer 3: Dense 2 executes in cycles [15603, 37269]
6:  $z_2 \leftarrow W_2a_1 + b_2$ 
7:   ▷ Layer 4: ReLU 2 executes in cycles [37270, 40259]
8:  $a_2 \leftarrow \max(0, z_2)$ 
9:   ▷ Layer 5: Output layer executes in cycles [40260, 118602]
10:  $z_o \leftarrow W_oa_2 + b_o$ 
11:  $\hat{y} \leftarrow \text{softmax}(z_o)$    ▷ Softmax output probabilities
12: return  $\hat{y}$ 

```

Fault Parameter	Minimum	Maximum	Step Size
Width	0	4000	100
Offset	0	4000	100
External Offset	0	118179	1
Repeat	1	5	1

TABLE I: Fault parameter search space.

goal of our work. We do not assume access to the cryogenic quantum hardware or the ability to directly perturb qubits; our focus is the ML component in the readout logic in the controller.

III. ATTACK IMPLEMENTATION

A. Attack Workflow

The ML-based quantum controller algorithm from [2] has been ported to C and implemented on ChipWhisperer Husky [17] to test the effect of voltage glitching on this algorithm. The algorithm is executed on a target Micro-Controller Unit (MCU), shown in Figure 1. The figure also summarizes the experimental loop. A host PC configures the ChipWhisperer Husky’s scope and glitch module and communicates with the MCU target that runs the ML algorithm. For each trial, we reboot and arm the target to ensure it is in a clean state. Then, we send one test input consisting of IQ data from [2], and inject a single glitch aligned to a trigger, and log the returned class plus device status (correct, misprediction, or reset or hang).

B. Faulting Parameter Search Space

In each voltage or clock fault experiment the following fault parameters are explored to find effective faults:

- **Width** - The width of a single glitch pulse.
- **Offset** - The offset within a clock cycle starting from the rising clock edge.
- **External Offset** - The number of clock cycles from the trigger until the glitch is performed.
- **Repeat** - The number of glitch pulses performed. Only applies to voltage faults.

The search space of these parameters is searched using Optuna [18], an optimization framework. In our experiments, Optuna is given the fault parameters as well a metric of success. The fault parameter search space is summarized in Table I. The objective maximizes the expected Hamming distance between the predicted 5-bit output and the ground truth, subject to a penalty for resets or hangs. To limit the searching time, we randomly selected test data corresponding to one of each of 32 classes and fault each one 3 times, resulting in 96 fault attempts at each tested combination of parameters. Thus, later in this work, success of a fault parameter is measured as number of faulty results out of 96 tested one.

C. Synchronization and Per-Layer Timing Windows

To attribute faults to specific neural network layers, we instrument trigger points around each layer (e.g., entry to `dense_1()`, `relu_1()`, etc.) and empirically measure the cycle ranges where each layer executes. We then restrict the external-offset search to these layer-specific windows (Algorithm 1), enabling controlled comparisons across layers.

IV. EXPERIMENTAL RESULTS

A. Successful Faults Across Neural Network Layers

We first present results of finding successful faults across the layers of the neural network responsible for error correction of the quantum computer readout. Figures 2 to 6 show the width, offset, and external offset of the successful faults we found. For each layer, the top-5 faulting configurations are also shown in Tables II to VI. These experiments focus on the *untargeted* faults: reducing the accuracy and increase the Hamming distance between predicted and true 5-bit strings, maximally causing the output to change, leading to incorrect interpretation of the quantum computation’s results.

We observe that all layers in the HERQULES neural network are susceptible to fault injection. The 3D plots demonstrate that for each layer, the successful faults can be found at variety of external offset. There is some clustering, e.g., *Layer 1: Dense 1* and *Layer 5: Output* tend to have many faults at offset close to the start of each of the layers (left-side of the graphs), while the other layers tend to have more faults clustered at higher external offset (right-side of the graphs).

Based on Tables II to VI, we observe a clear pattern: early layers (*Layer 1: Dense 1* and *Layer 2: ReLU 1*) exhibit the highest fault success rates across the top configurations (up to 27/96), whereas later layers show substantially fewer successful faults (around 5/96). Thus faults at earlier layers induce mispredictions in a large fraction of runs, whereas later stages (e.g., output) are much harder to fault reliably. This is consistent with the intuition that dense layers execute long MAC chains (large timing surface) and that downstream non-linearities can amplify early numerical perturbations into categorical output collapse [15].

The results also show that attackers can easily find fault injection points, and many of these results in successful *untargeted* attacks. We find interesting observation that the width

and offset have typically limited ranges of successful values (between 2400 to 2800). Meanwhile, the best external offset is layer-dependent, although many faults can be found at variety of external offsets.

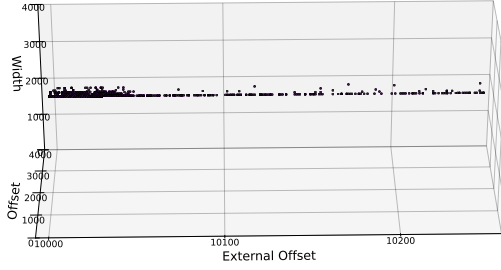


Fig. 2: Points where successful voltage glitches were found in *Layer 1: Dense 1* layer.

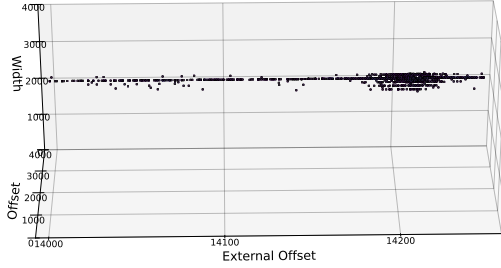


Fig. 3: Points where successful voltage glitches were found in *Layer 2: ReLU 1* layer

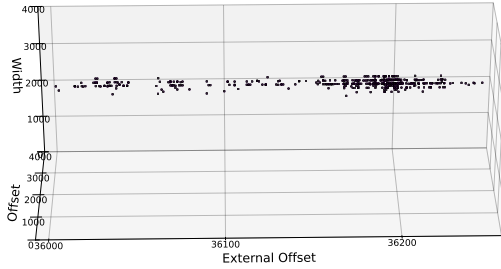


Fig. 4: Points where successful voltage glitches were found in *Layer 3: Dense 2* layer

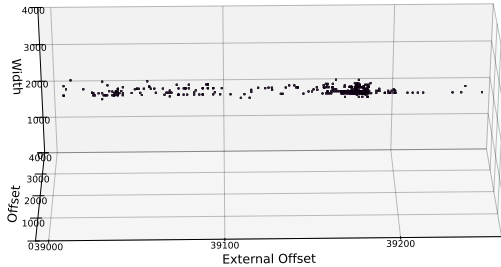


Fig. 5: Points where successful voltage glitches were found in *Layer 4: ReLU 2* layer

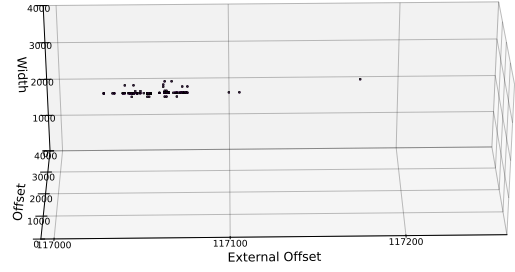


Fig. 6: Points where successful voltage glitches were found in *Layer 5: Output* layer

TABLE II: Best fault-inducing configuration per layer in the 5-layer network targeting *Layer 1: Dense 1* layer. The No. of Faults column corresponds to the number of successful faults observed out of 96 repetitions.

Configuration	Width	Offset	External Offset	Repeats	No. of Faults
1	2400	2400	10026	2	13
2	2400	2400	10021	2	13
3	2400	2400	10010	2	12
4	2400	2400	10013	2	12
5	2400	2500	10027	2	12

TABLE III: Best fault-inducing configuration per layer in the 5-layer network targeting *Layer 2: ReLU 1* layer. The No. of Faults column corresponds to the number of successful faults observed out of 96 repetitions.

Configuration	Width	Offset	External Offset	Repeats	No. of Faults
1	2700	2600	14208	5	27
2	2700	2600	14207	5	24
3	2700	2600	14209	5	23
4	2700	2600	14206	5	22
5	2700	2600	14211	5	22

TABLE IV: Best fault-inducing configuration per layer in the 5-layer network targeting *Layer 3: Dense 2* layer. The No. of Faults column corresponds to the number of successful faults observed out of 96 repetitions.

Configuration	Width	Offset	External Offset	Repeats	No. of Faults
1	2600	2800	36170	5	5
2	2700	2600	36116	5	5
3	2500	2600	36194	1	4
4	2700	2600	36210	4	4
5	2600	2800	36194	4	4

TABLE V: Best fault-inducing configuration per layer in the 5-layer network targeting *Layer 4: ReLU 2* layer. The No. of Faults column corresponds to the number of successful faults observed out of 96 repetitions.

Configuration	Width	Offset	External Offset	Repeats	No. of Faults
1	2500	2400	39175	5	7
2	2500	2400	39180	5	7
3	2500	2400	39174	5	6
4	2500	2500	39177	5	6
5	2500	2400	39637	5	6

B. Fault Impact on Specific Readout Values

Beyond untargeted degradation, we examined how the best faulting configurations can bias outputs toward attacker-chosen targets (e.g., forcing specific 5-bit strings). The results are shown in Figures 7 to 12.

TABLE VI: Best fault-inducing configuration per layer in the 5-layer network targeting *Layer 5: Output* layer. The No. of Faults column corresponds to the number of successful faults observed out of 96 repetitions.

Configuration	Width	Offset	External Offset	Repeats	No. of Faults
1	2500	2400	117065	5	4
2	2500	2400	117044	4	3
3	2500	2400	117047	5	3
4	2500	2500	117064	5	3
5	2500	2400	117063	5	3

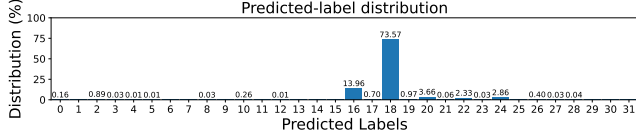


Fig. 7: Distribution of classification of outputs for input 10010 under no fault attack.

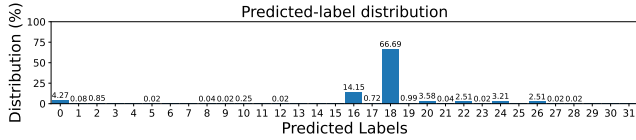


Fig. 8: Distribution of classification of outputs for input 10010 when faulting *Layer 1: Dense 1* layer.

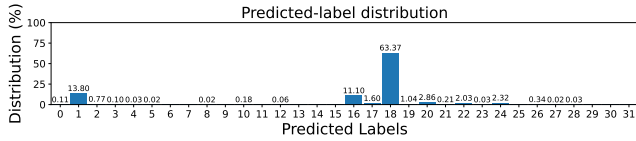


Fig. 9: Distribution of classification of outputs for input 10010 when faulting *Layer 2: ReLU 1* layer.

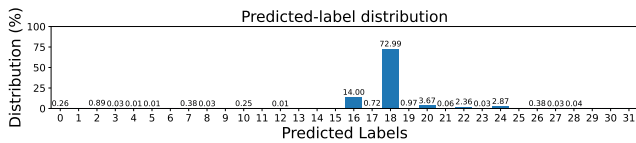


Fig. 10: Distribution of classification of outputs for input 10010 when faulting *Layer 3: Dense 2* layer.

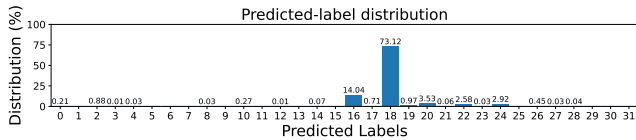


Fig. 11: Distribution of classification of outputs for input 10010 when faulting *Layer 4: ReLU 2* layer.

In the figures we show the results of applying top faulting configuration from each layer onto a randomly selected input

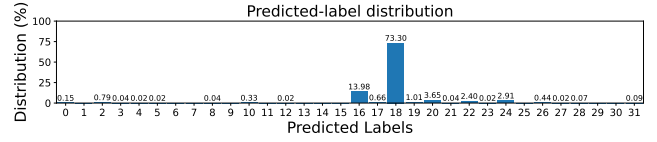


Fig. 12: Distribution of classification of outputs for input 10010 when faulting *Layer 5: Output* layer.

from the data set. The randomly selected input corresponds to IQ data for readout that should be the binary 10010, this corresponds to integer value 18. Due to known issue with the device tested by HERQULES to collect the data, the bit 1 has high level of noise, thus even with no fault attack, shown in Figure 7 the ML algorithm outputs 18 with high probability, but also outputs 16 quite often since bit 1 is noisy and readout generates 10000 instead of 10010.

Most interestingly, we observe that by applying this fault to *Layer 2: ReLU 1* layer, we can generate output 1 or binary 00001 almost 20% of time when fault attack is applied. We also observe that the correct output 18 is reduced from about 75% to about 60% when attacking layers 1 and 2. Meanwhile, the reduction is much less when attacking layers 3, 4, and 5. This is consistent with the prior observation that the faults are most successful on early layers.

Our results demonstrate that it is much more difficult to achieve *targeted* steering: biasing corrected outputs toward attacker-chosen bitstrings (specific 5-bit classes), enabling adversarial manipulation of the results of the computation that are received by the users. While prior work demonstrated in other types of ML algorithms the feasibility of such adversarially steering [15], the impact on HERQULES is much less when selecting random input. Note that if attacker knows the input, he or she can perform extended testing to find faulting parameters that affect just that input and realize the targeted steering. This is left as future work.

V. DISCUSSION

A. Why are dense layers especially vulnerable?

Our results indicate that dense layers provide high-yield fault surfaces: the best configurations induce mispredictions frequently in the dense layers, compared to ReLU layers. Further, the last output layer is harder to fault reliably. A plausible explanation is that dense layers execute long multiply-accumulate (MAC) chains and memory accesses, expanding the temporal window in which a transient voltage fault can perturb intermediate values or control flow. In addition, small numerical perturbations injected early can cascade into categorical output changes (including mode collapse), consistent with prior fault-injection studies showing that deep neural network inference can suffer sharp accuracy degradation under transient faults [15].

B. What are security implications for quantum readout pipelines?

Unlike many ML deployments where mispredictions degrade only application quality, readout correction sits directly on the quantum-classical interface and can influence decoders, calibration loops, and any downstream classical control that depends on measurement outcomes. In cloud settings, these risks align with broader concerns that quantum computations may rely on untrusted or compromised classical infrastructure [3], [4], [5]. Our findings suggest that ML readout correction should be treated as a security-critical primitive: a physical attacker can potentially steer corrected readout strings toward specific bit patterns, not merely increase noise.

C. What are possible defenses?

We recommend lightweight, deployment-friendly defenses inspired by established fault-attack countermeasures [12], [19]: (1) redundant inference (majority voting) on a subset of shots; (2) cross-checking with a simpler discriminator (e.g., matched-filter baseline) and rejecting inconsistent outcomes; (3) runtime sanity checks on logits or entropy and range checks on intermediate activations; (4) hardware monitors (brown-out or glitch detectors and clock monitors) configured to reset and flag anomalous operation; and (5) randomized timing (jitter) for layer execution to reduce precise synchronization.

VI. RELATED WORK

A. Readout Error Mitigation and ML for Quantum Readout

Measurement-error mitigation commonly relies on calibrated assignment models and classical post-processing [9], [10]. More recent work explores ML-based readout improvement using deep discriminators for multiplexed readout [1] and scalable, hardware-efficient ML readout architectures [2], as well as other deep-learning-based approaches to readout error correction [11]. The existing work on readout and ML has not considered security attacks on the ML and its operation.

B. Fault Injection Against ML

Fault attacks on embedded systems have a long history [20], [12]. Recent studies demonstrate that DNN inference can be highly vulnerable to fault injection, where transient faults can induce severe accuracy degradation and even targeted outcomes [15]. While fault-injection attacks are well known, they have not been considered in context of ML and quantum computer readout.

C. Security of the Quantum Stack

Work on quantum security increasingly emphasizes threats arising from the attacks on quantum computers [6]. Attacks have been evaluated from the quantum software layer, where attacker can attack specific algorithms [21], to the hardware level, where attackers can attack the control pulses driving qubits [3]. Within quantum computing devices, attacks have focused mainly on crosstalk [22] where operation of some qubits affects near-by qubits inducing incorrect computation. Our work on fault injection was inspired by a proposed

classification [5] of fault injection attacks in quantum computer. We are the first to actually enact such fault injection on quantum computer controller and the ML algorithms it runs. Closest work to ours on security of quantum computer controllers has focused on side-channel attacks [4], but not of fault injection. Our work is first to provide an empirical, hardware-backed case study focused on fault-injection on a concrete ML component in the readout logic and quantum computer controller.

VII. CONCLUSION

We presented the first voltage-glitch fault injection study against an embedded ML-based quantum readout error-correction model. By timing glitches to layer-specific windows and using automated parameter search, we found many fault-injection vulnerability in all the layers of the ML model. These results suggest that ML readout correction should be treated as a security-critical primitive and defenses need to be integrated into quantum readout pipelines. Future work can include extending this work to EM fault injection and clock glitching attacks, plus design of defenses.

ACKNOWLEDGEMENTS

This work was supported in part by National Science Foundation grant 2245344.

REFERENCES

- [1] B. Lienhard *et al.*, “Deep neural network discrimination of multiplexed superconducting qubit states,” *Physical Review Applied*, 2022.
- [2] S. Maurya, C. N. Mude, B. Lienhard, W. D. Oliver, and S. Tannu, “Scaling qubit readout with hardware efficient machine learning architectures,” in *Proceedings of the 50th Annual International Symposium on Computer Architecture (ISCA)*, 2023.
- [3] T. Trochatos *et al.*, “Dynamic pulse switching for protection of quantum computation on untrusted clouds,” in *IEEE International Symposium on Hardware Oriented Security and Trust (HOST)*, 2024.
- [4] C. Xu, F. Erata, and J. Szefer, “Quantum computer fault injection attacks,” in *2024 IEEE International Conference on Quantum Computing and Engineering (QCE)*, pp. 331–337, Sept. 2024.
- [5] C. Xu, F. Erata, and J. Szefer, “Classification of quantum computer fault injection attacks,” arXiv:2309.05478, 2023.
- [6] S. Ghosh *et al.*, “A primer on security of quantum computing hardware,” arXiv:2305.02505, 2023.
- [7] B. Nachman, M. Urbanek, W. A. de Jong, and C. W. Bauer, “Unfolding quantum computer readout noise,” *npj Quantum Information*, vol. 6, no. 1, p. 84, 2020.
- [8] I. Rojko, D. Layden, P. Cappellaro, J. Home, and F. Reiter, “Bias in error-corrected quantum sensing,” *Physical Review Letters*, vol. 128, no. 14, p. 140503, 2022.
- [9] F. B. Maciejewski, Z. Zimboras, *et al.*, “Mitigation of readout noise in near-term quantum devices by classical post-processing based on detector tomography,” *Quantum*, vol. 4, p. 257, 2020.
- [10] P. D. Nation, H. Kang, N. Sundaresan, and J. M. Gambetta, “Scalable mitigation of measurement errors in near-term quantum devices,” 2021.
- [11] J. Kim *et al.*, “Quantum readout error mitigation via deep learning,” 2021.
- [12] A. Barenghi, L. Breveglieri, I. Koren, D. Naccache, and F. Regazzoni, “Fault injection attacks on cryptographic devices: Theory, practice, and countermeasures,” *Proceedings of the IEEE*, vol. 100, no. 11, pp. 3056–3076, 2012.
- [13] M. Eslami *et al.*, “A survey on fault injection methods of digital integrated circuits,” *Integr. VLSI J.*, 2020.
- [14] A. Gangolli *et al.*, “A systematic review of fault injection attacks on IoT devices,” *Electronics*, 2022.

- [15] J. Breier, Z. Houar, *et al.*, “Practical fault attack on deep neural networks,” 2018.
- [16] J. Heinsoo, C. K. Andersen, A. Remm, S. Krinner, T. Walter, Y. Salathé, S. Gasparinetti, J.-C. Besse, A. Potočnik, A. Wallraff, *et al.*, “Rapid high-fidelity multiplexed readout of superconducting qubits,” *Physical Review Applied*, vol. 10, no. 3, p. 034040, 2018.
- [17] C. O’Flynn and Z. D. Chen, “Chipwhisperer: An open-source platform for hardware embedded security research,” in *Constructive Side-Channel Analysis and Secure Design (COSADE)*, vol. 8622 of *LNCS*, pp. 243–260, Springer, 2014.
- [18] T. Akiba, S. Sano, T. Yanase, T. Ohta, and M. Koyama, “Optuna: A next-generation hyperparameter optimization framework,” 2019.
- [19] N. Moro *et al.*, “Experimental evaluation of two software countermeasures against fault attacks,” 2014.
- [20] D. Boneh, R. A. DeMillo, and R. J. Lipton, “On the importance of checking cryptographic protocols for faults,” in *EUROCRYPT*, 1997.
- [21] K. Tessma, H. Kukina, and J. Szefer, “Recovering qsvt polynomials from side-channel information on quantum computers,” in *International Conference on Computer Design, ICCD*, November 2025.
- [22] S. Deshpande, C. Xu, T. Trochatos, H. Wang, F. Erata, S. Han, Y. Ding, and J. Szefer, “Design of quantum computer antivirus,” in *Proceedings of the International Symposium on Hardware Oriented Security and Trust, HOST*, May 2023.